Optics Communications 447 (2019) 6–12

Contents lists available at ScienceDirect

Optics Communications

journal homepage: www.elsevier.com/locate/optcom

Q-switched and mode-locked thulium doped fiber lasers with nickel oxide film saturable absorber

M.F.M. Rusdi [a], A.H.A. Rosol [a], M.F.A. Rahman [a,d], M.B.H. Mahyuddin [a], A.A. Latiff [c], H. Ahmad [b], S.W. Harun [a,*], M. Yasin [e]

[a] Photonics Engineering Laboratory, Department of Electrical Engineering, Faculty of Engineering, University of Malaya, 50603 Kuala Lumpur, Malaysia
[b] Photonics Research Centre, University of Malaya, 50603 Kuala Lumpur, Malaysia
[c] Faculty of Electronic and Computer Engineering, Universiti Teknikal Malaysia Melaka, 76100 Hang Tuah Jaya, Melaka, Malaysia
[d] Fakulti Teknologi Kejuruteraan Elektrik & Elektronik, Universiti Teknikal Malaysia Melaka, 76100 Hang Tuah Jaya, Melaka, Malaysia
[e] Department of Physics, Faculty of Science and Technology, Surabaya, Indonesia

ARTICLE INFO

Keywords:
Fiber lasers
Pulsed laser
Q-switching
Mode-locking
Thulium-doped fiber laser
Nickel oxide

ABSTRACT

A passively Q-switched and mode-locked fiber laser based on thulium-doped fiber laser (TDFL) cavity was demonstrated utilizing nickel oxide (NiO) nanoparticles as a saturable absorber (SA). The NiO synthesis was carried out by using a facile sonochemical method and the prepared NiO thin film was sandwiched between two optical fiber ferrule connectors in the TDFL ring cavity. By controlling the loss and gain in the cavity, stable Q-switching operation was obtained. The repetition rate and pulse width were tunable from 6.71 kHz to 19.58 kHz and from 9.16 μs to 4.24 μs respectively, at different pump powers, ranging from 528 mW to 711 mW. The Q-switched TDFL was centered at 1900.52 nm and had maximum pulse energy and slope efficiency of 0.31 μJ and 2.58%, respectively. On the other hand, self-starting mode-locked TDFL was achieved by employing 10 m scandium-doped fiber into the ring cavity and remained stable within a pump power range of 821–967 mW. The TDFL mode-locked had a central wavelength of 1928.81 nm, at a threshold pump power of 821 mW. The repetition rate and pulse width were 8.10 MHz and 61.27 ns, respectively, while the slope efficiency was measured to be 2.20 %.

1. Introduction

Fiber lasers operating in the mid-infrared spectral region around 2 μm have attracted great attention among researchers due to their potential applications in light detection and ranging (LIDAR), telecommunication, plastic welding and spectroscopy [1–3]. Additionally, in the field of medical surgery such as endourology (coagulation or tissue cutting), the thulium and holmium-doped fiber laser has been claimed to be the most suitable laser source as compared to the erbium and ytterbium-doped fiber lasers, mainly because of their operating wavelengths, which have high absorption coefficient in water and gases. The wavelength absorption coefficients for the thulium and holmium in water are 1.94 μm at 114 cm^{-1} and 2.12 μm at 36 cm^{-1}, respectively, as reported by Nathaniel et al. [4]. The technology operating near this wavelength fall into the 'eye-safe laser' category, which provides a unique advantage to many applications [5]. Thulium and holmium ions based active fibers have a broad gain bandwidth and thus they are very suitable for ultrashort pulses generation as well as to produce laser with wideband wavelength tuning [6]. For instance, by utilizing the full gain bandwidth (>200 nm) of thulium-doped fiber, sub 30 fs mode-locking pulses train can be directly generated from an oscillator [7].

There are two techniques that can be used to produce Q-switching and mode-locking pulses, namely active and passive. The active technique typically uses external acousto-optic modulators to actively control and modulate the intra-cavity light. These devices are quite bulky, complex and expensive in fabrication [8,9]. Compared to the active technique, the passive technique requires no external pulse triggering signal, and thus, is relatively lower in cost and much simpler in fabrication and set-up. It can be simply obtained by employing a saturable absorber (SA) device in the cavity. The SA modulates light by exploiting its inherent linear and non-linear optical absorption properties [10].

There are various types of SA; artificial and real, including the nonlinear polarization rotation (NPR), nonlinear optical loop mirror (NOLM), nonlinear amplifying loop mirror (NALM), semiconductor saturable absorber mirror (SESAM), carbon nanotube (CNT), ion-doped crystal and few others published recently [11–13]. SESAMs were quite famous in the early years due to their stability, high flexibility and fast amplitude modulation [14–16]. However, SESAMs have several disadvantages including quite bulky for fiber lasers, expensive, and complex in fabrication and packaging. In addition to that, they also have limited optical response bandwidth. The NPR, NOLM and NALM

* Corresponding author.
E-mail addresses: swharun@um.edu.my (S.W. Harun), yasin@fst.unair.ac.id (M. Yasin).

https://doi.org/10.1016/j.optcom.2019.04.083
Received 26 February 2019; Received in revised form 5 April 2019; Accepted 29 April 2019
Available online 4 May 2019

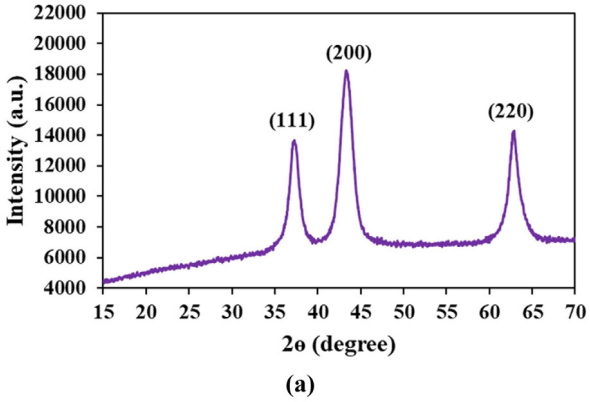

(a)

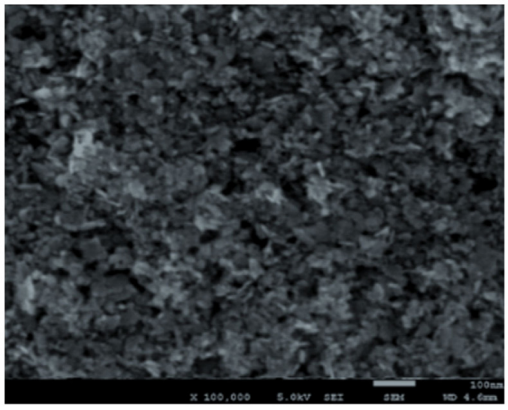

(b)

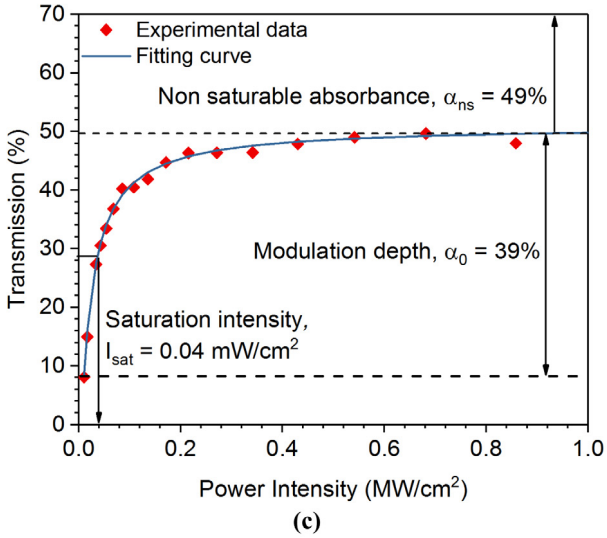

(c)

Fig. 1. Characteristics of NiO film SA (a) XRD analysis (b) image of FESEM (c) nonlinear transmission curve.

on the other hand, are vulnerable to external disturbances and not always self-starting. Therefore, to overcome this problem, researchers have proposed new materials which are relatively cheaper and easier to fabricate such as the zero-dimensional (0D) and two-dimensional (2D) materials [17,18]. The 2D materials such as graphene, topological insulators (TIs), transition-metal dichalcogenides (TMDs) and black phosphorus (BP) were quite popular in the last few years, owing to their unique characteristic; strong intra-layer covalent bonding and weak inter-layer van der Waals force [18–20]. For example, BP was

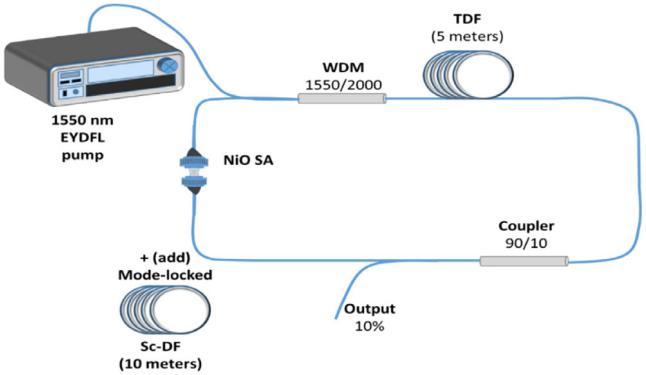

Fig. 2. The proposed configuration of the TDFL for generating Q-switching and mode-locking pulses using the newly developed NiO based SA.

reported to have a broadband optical response for infrared and mid-infrared optoelectronics, as its properties show similarity with the graphene, such as single elemental component and direct band-gap, making BP one of the most popular materials used as SA [21]. However, BP is a hydrophilic material and thus, easy to dissolve in the humid air. Besides BP, molybdenum disulfide (MoS_2) and titanium dioxide (TiO_2) thin film are also capable of modulating light in the region of 2 μm [22,23]. Nickel oxide (NiO) has been a successful SA in producing Q-switched and mode-locked pulse fiber laser for 1 μm and 1.55 μm region [24,25]. The unique properties of NiO such as low saturation intensity, appropriate modulation depth as well as suitable band-gap energy of 3.6–4.0 eV [26], allows it to be used as an alternative SA in the 2 μm region.

In this paper, Q-switched and mode-locked TDFLs were demonstrated by a passive technique using NiO film SA. The NiO film was prepared via a facile sonochemical method. A small part of NiO thin film (1 mm × 1 mm) was sandwiched between two fiber connectors. By inserting the NiO film SA into the laser cavity, a stable Q-switched laser centered at 1928.81 nm was obtained. The Q-switched pulse had a tunable repetition rate within 6.71–19.58 kHz. Additionally, by adding 10 m scandium-doped fiber (Sc-DF) into the pre-configured cavity, self-starting mode-locked laser centered at 1900.51 nm could be achieved. The mode-locked pulse had a repetition rate of 8.10 MHz. Based on our observations, this is the first demonstration, using NiO thin film SA for producing Q-switching and mode-locking pulses operating in the 2 μm region.

2. Fabrication and characterization of the SA

The fabrication process of the NiO nanoparticle involves two steps; first, the formation of nickel nanoparticle powder, and secondly the formation of the thin film containing the nickel nanoparticle. At first, nickel chloride hexahydrate was dissolved in deionized water (50 ml) and later, this mixture was put at constant stirring for 10 min. Then, the prepared solution was further added with sodium hydroxide solution. The mix-solution was sonicated utilizing a horn type sonicator for around 1 h with an amplitude setting of 60%. The product of the sonication process was later centrifuged and washed for several times using distilled water. Next, we calcinated the sample at 350 °C in an electrical furnace to form the NiO nanoparticle particle. On the other hand, the host material was prepared by dissolving 1 g of polyethylene oxide (PEO) in distilled water. Later, the previously prepared NiO nanoparticle powder was added into the host solution and was stirred for 2 h. Then, the complete mixture solution was poured into a petri-dish and left to dry at the room temperature for 24 h, to form the solid NiO thin film.

To analyze the NiO nanoparticle, we performed various measurements such as X-ray diffraction (XRD), field emission scanning electron

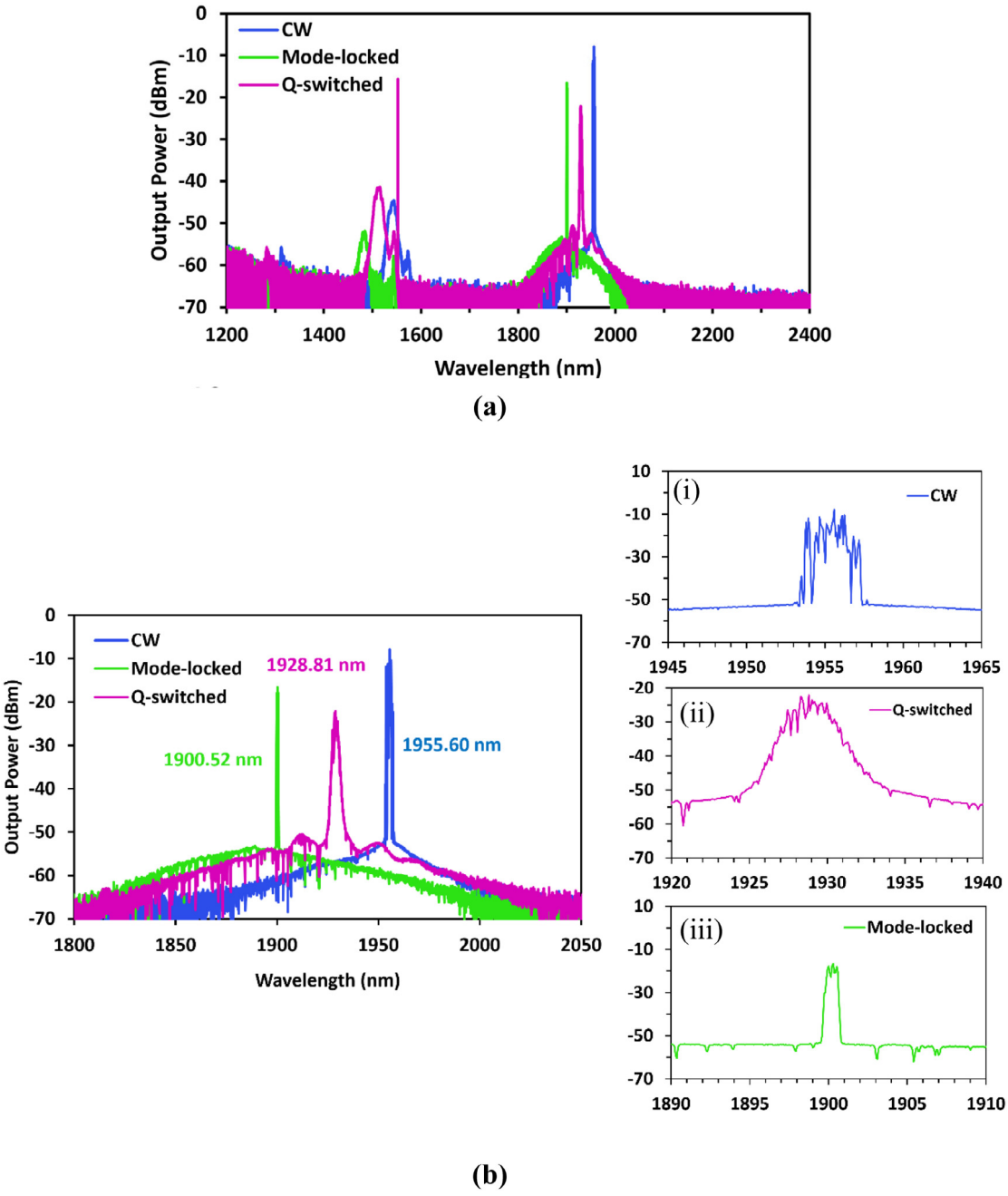

Fig. 3. Output spectra of the CW, Q-switched and mode-locked TDFLs at the respective threshold pump powers, at (a) 1200–2400 nm span, (b) 1800–2050 nm span, while the insets (i-iii) show the individual CW, Q-switched and mode-locked TDFL spectrum in detail.

microscopy (FESEM) and non-linear. Fig. 1(a) shows the measured XRD profile of the nanoparticle SA. As seen in the figure, there are three peaks, which correspond to three different vibrational modes of the NiO plane crystalline; (111), (200), and (220) at 37.28°, 43.28° and 62.88°, respectively. These crystalline planes are corresponding to the face-centered cubic structure of the NiO. The FESEM image of the NiO nanoparticle as shown in Fig. 1(b) depicts a considerably high density of nanoparticles. The nonlinear optical absorption of the SA was also measured based on the twin balance detector method. In the measurement, a homemade mode-locked source with a central wavelength of 1560 nm, 1 MHz repetition rate and 1.25 ps pulse width was utilized. The laser source was connected to a variable optical attenuator and then into a 3 dB coupler to split the beam. One part of the beam was launched into the film and another part was used as a reference. The transmitted power was measured by using an optical power meter so that the SA nonlinear transmission profile can be plotted as shown in Fig. 1(c). The experimental data then is fitted with a simple saturable absorption curve of transmission, $T(I) = 1 - \alpha_0 x\ exp(-I/I_{sat}) - \alpha_{ns}$; where $T(I)$ is the transmission, α_0 is the modulation depth, I is the input intensity, I_{sat} is the saturation intensity, and α_{ns} is the non-saturable absorbance [27]. The result indicates that the SA has a modulation depth of 39%, non-saturable absorbance of 49% and saturation intensity of 0.4 MW/cm^2. The measured modulation depth is examined to be comparable with the others SA [28,29].The fabricated NiO film has a thickness of around 40 μm.

3. Laser configuration

The schematic diagram of the proposed TDFL is illustrated in Fig. 2. The laser cavity has a total fiber length of 13 m where the longest

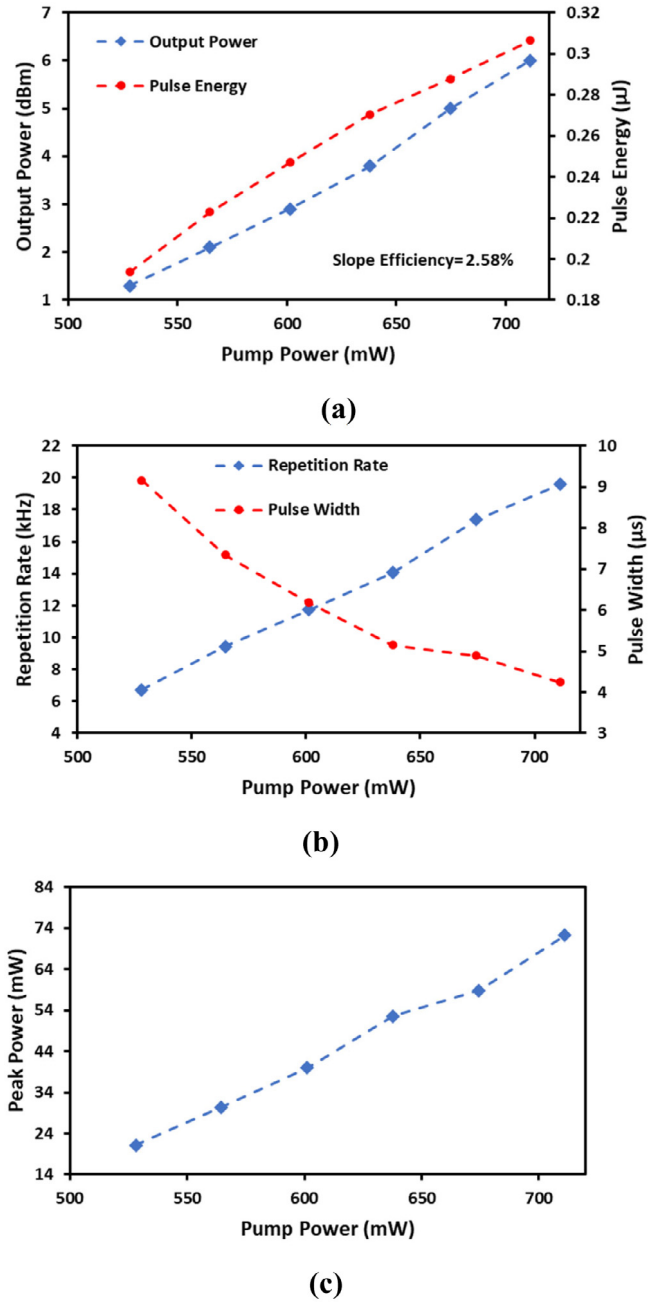

Fig. 4. Q-switching performances of the TDFL with a variation of pump power from 528 to 711 mW (a) output power and pulse energy (b) repetition rate and pulse width (c) peak power.

part in the cavity belongs to the 5 m long Thulium-doped fiber (TDF), which acts as the gain medium. The TDF used in this experiment is Nufern SM-TSF-9/125 commercial fiber and has a core diameter of 9 μm and a numerical aperture of 0.15. The thulium ion absorption of the fiber is about 9.3 dB/m and 27 dB/m at 1180 nm and 793 nm, respectively. The TDF has a group velocity dispersion (GVD, β_2) of approximately −86.8 ps^2/km at 1990 nm wavelength. The GVD data of the specified manufacturing batch of the TDF was obtained from the fiber glass manufacturer. The TDF gain medium is pumped by a fiber laser operating at 1552 nm from a homemade erbium ytterbium-doped fiber laser (EYDFL) through a wavelength division multiplexer (WDM). A 90/10 optical coupler in the ring cavity retains 90% of the oscillating laser within the ring cavity while diverting out the rest 10% for various optical measurements and analysis. The SA was prepared by cutting a small piece (1 mm x 1 mm) of the NiO-PVA thin film. The SA film was then sandwiched between two fiber ferrules and inserted into the laser cavity. The insertion loss of the SA film was measured to be around 1.5 dB. We did not measure the polarization dependent loss, as the integration of polarization controller that usually used to change the optical polarization state in the laser cavity did not enhance the pulsed laser stability nor the pulse width. The output laser optical spectrum was observed via an optical spectrum analyzer (OSA, YOKOGAWA-AQ6375). The generated pulse signal in the time domain and frequency domain were analyzed via a 500 MHz digital oscilloscope and 7.8 GHz RF spectrum analyzer (Anritsu), respectively. Both pieces of equipment were pre-connected with an InGaAs based 7 GHz photodetector (PD). An additional element of 10 m long Sc-DF was incorporated into the cavity to assist the mode-locked laser generation by providing a sufficient intracavity dispersion and nonlinearity effect. This is because for a stable mode-locked operation, both dispersion and nonlinearity to be well balanced. The Sc-DF used in this work has a core diameter of 7.5 μm with background loss 50~75 dB/km at 1285 nm. The numerical aperture and GVD parameter are 0.12 and −127 ps^2/km, respectively. Without the Sc-DF, only Q-switching pulses could be observed.

4. Result and discussion

Fig. 3(a) depicts the output spectrum of the proposed TDFL in 1200 nm wavelength span when it is operating at three different regimes; continues wave (CW), Q-switching and mode-locking modes. In the experiment, the output spectrum was obtained at the respective threshold pump powers. Without employing any SA in the cavity, first, the CW laser (centered at 1955.60 nm) is established, as the pump power raised above the CW threshold of 418 mW. Fig. 3(b) shows the enlarged image of the related lasing spectra taken within a span of 250 nm taken at 0.05 nm OSA resolution, while the inset of Fig. 3(b) shows the individual spectrum; the CW, Q-switched and mode-locked TDFL in detailed views. By inserting the NiO-SA into the ring cavity, and further elevates the pump power to 528 mW, the CW laser transits into Q-switched laser, that peaks at 1928.81 nm wavelength. Self-generated mode-locked, centered at 1900.52 nm wavelength stably appears when an additional 10 m Sc-DF is integrated into the ring cavity at the threshold pump power of 821 mW. The existence of some ripples in the CW laser is due to modes competition that arises at the initial stage of CW. When the pump power is increased, the number of laser modes also increases due to the increase in the level of the gain profile. As illustrated in the inset of Fig. 3(b), the output spectrum of the Q-switched is much broader than the CW and mode-locked laser spectrum. The 3 dB spectral bandwidth of the Q-switching pulses is about 0.28 nm, while the CW and mode-locked lasers are 0.07 nm and 0.14 nm, respectively. Also, the laser peak wavelengths are observed to be shifting to the nearer wavelength, when the CW laser transits into the Q-switched and mode-locked laser, respectively. This phenomenon is attributed to the change in cavity loss as a result of the SA insertion. The wavelength shift for the mode-locked is seen to be more significant than the Q-switched laser, due to additional insertion of Sc-DF into the cavity [26]. Higher pump power is needed to attain laser oscillation in this higher loss laser cavity; the system technically will compensate for this loss by shifting the peak wavelength towards the area with a higher gain.

Fig. 4 depicts the Q-switching performance of the TDFL, which was observed as the pump power increased from 528 mW to 711 mW. As shown in Fig. 4(a), the output power increases almost linearly from 1.3 mW to 6 mW, corresponding to a slope efficiency of 2.58%. At the same time, the pulse energy also increases from 0.19 μJ to 0.31 μJ, almost in the same trend with the output power. The existence of residual pump (as shown in the Q-switched spectrum as in Fig. 3(a)) was taken into consideration when calculating the output power and pulse energy. It was done by deducting certain output power value corresponding to the residual pump. Fig. 4(b) shows the repetition rate and pulse width of

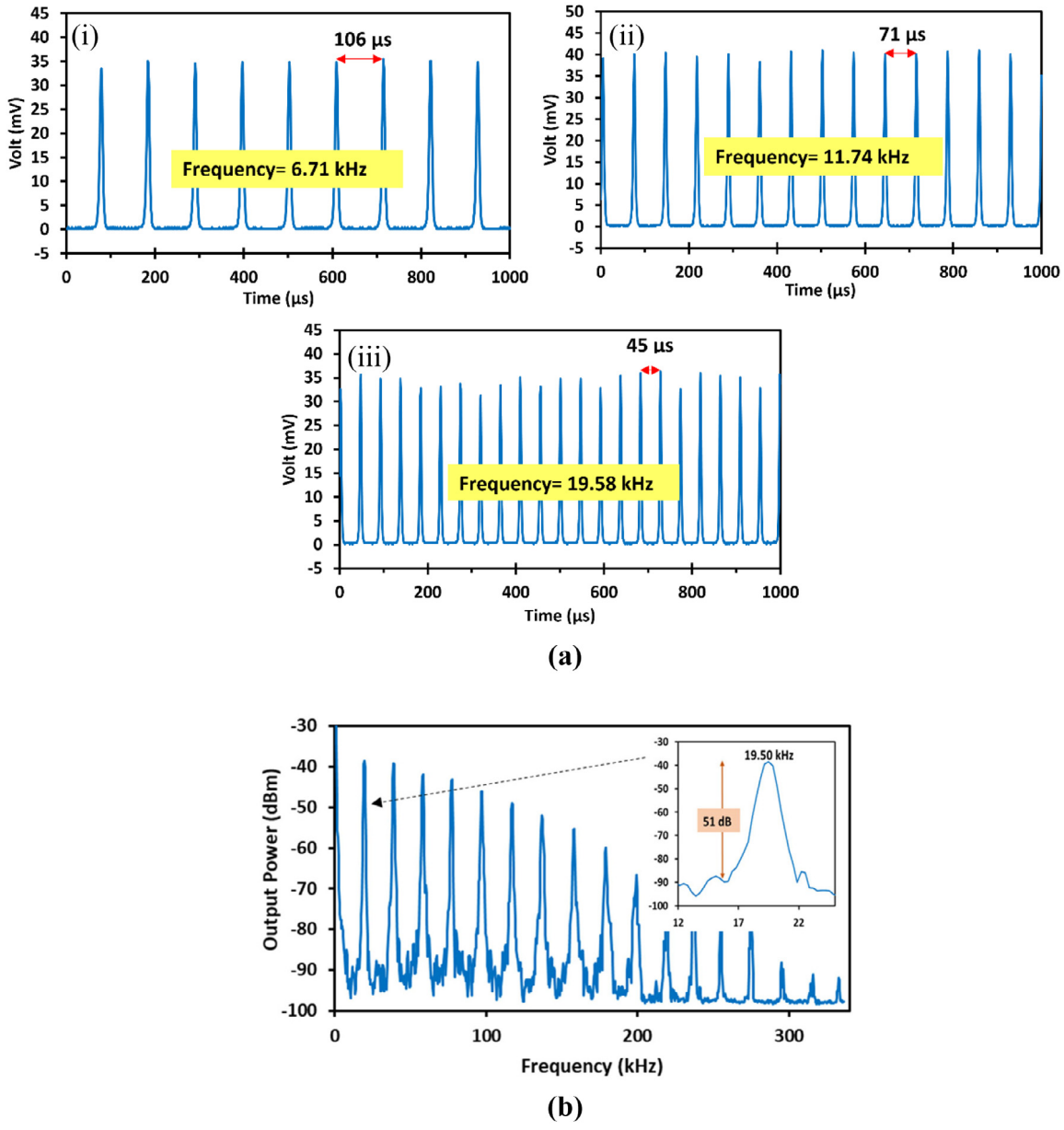

Fig. 5. Q-switched TDFL characteristics. (a) temporal performance of the pulsed laser at (i) 528 mW, (ii) 601 mW and (iii) 711 mW pump power, (b) frequency domain of the pulsed laser at the maximum pump power of 711 mW with the inset showing the fundamental frequency in detail view.

the Q-switched TDFL against the pump power. The repetition rate starts at 6.71 kHz and climbs-up to 19.58 kHz, as the pump power elevated to a maximum of 711 mW. Beyond this pump power, no pulse could be observed. As the repetition rate increases, the pulse width reduces from 9.16 µs to 4.24 µs. Fig. 4(c) plots the peak power in corresponds to the increasing pump power. As seen in the figure, the peak power raises from 21.55 mW to a maximum of 72.27 mW.

Fig. 5 shows the temporal characteristics of the Q-switched TDFL. The typical pulses train observed at 528 mW pump power is illustrated in Fig. 5(a)(i). It shows a quite stable pulses pattern, depicting an almost consistent repetition rate of 6.71 kHz with a corresponding peak to peak separation (pulse period) of 106 µs. When the pump power elevated further to 601 mW, the repetition rate increases up to 11.74 kHz, while the pulse period shrinks to 71 µs (Fig. 5(b)(ii)). As the pump power further increased up to 711 mW, as in Fig. 5(a)(iii), the pulses train becomes more intense, resulting in the higher repetition rate of 19.58 kHz, with a corresponding pulse separation of 45 µs. These phenomena, where the pulse frequency grows larger with the increase of pump power, as illustrated in Fig. 5(a)(i–iii), agrees well with the typical Q-switched laser characteristic. As more pump light is given into the cavity, more gain is available to saturate the SA, thus, the repetition rate becomes faster, while the pulse width becomes narrower. The Q-switched laser ceased to exist as the pump power raised beyond 711 mW. The experiment was further examined by decreasing the pump power from 711 mW to the Q-switching threshold pump power of 528 mW. Within this range of pump power, similar pulsed laser characteristics as reported earlier could always be obtained, indicating that the Q-switched laser was stable. This also proved that the laser operation was conducted below than the film SA thermal damage threshold. Fig. 5(b) shows the frequency domain of the Q-switched laser at the maximum pump power of 711 mW. The fundamental frequency is 19.50 kHz, while the signal to noise ratio (SNR) as depicted in the inset of Fig. 5(b), is measured as 51 dB.

Fig. 6 shows the mode-locking performance of the proposed TDFL as pump power was increased from 821 mW to 967 mW. No pulsed laser could be seen as we removed the SA film, which verifies that the

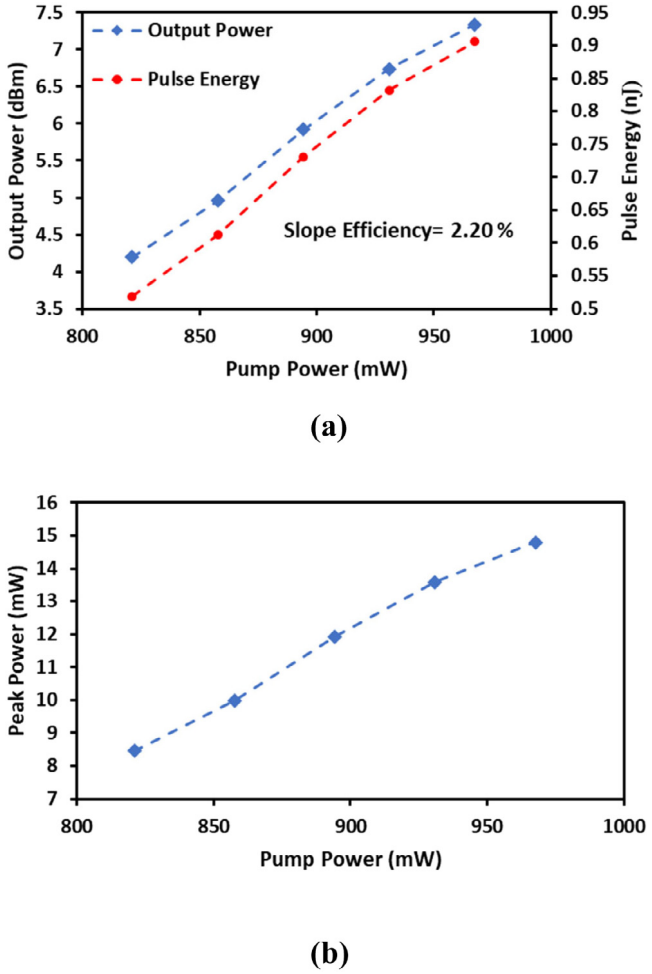

Fig. 6. Mode-locked TDFL performances at various pump powers, 821–967 mW (a) output power and pulse energy (b) peak power.

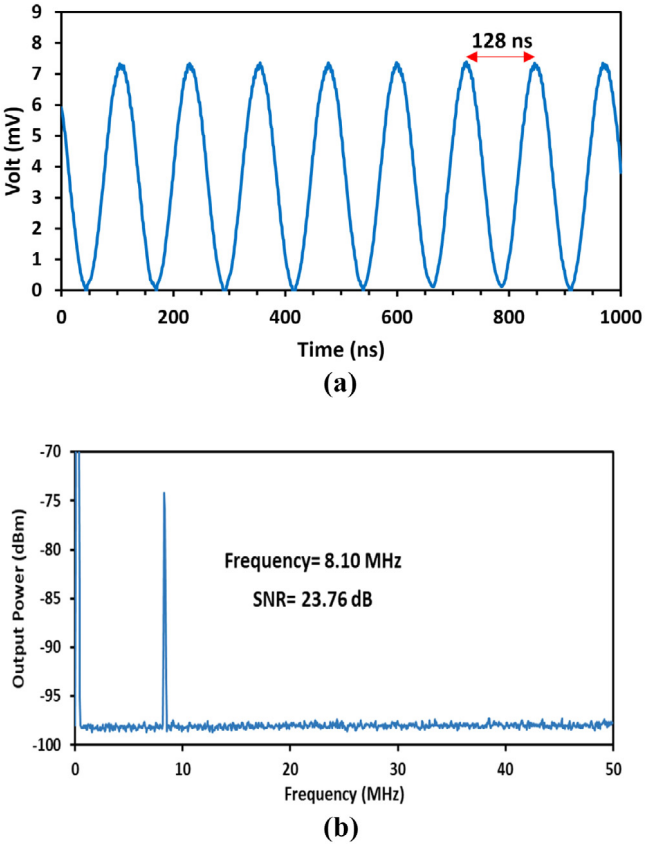

Fig. 7. TDFL mode-locked characteristics at the maximum pump power of 967 mW (a) temporal performance (b) frequency domain.

NiO film plays a significant role in starting and stabilizing the pulses train. As seen in Fig. 6(a), the output power increases almost linearly from 4.20 mW to 7.34 mW and this equivalent to a slope efficiency of 2.20%. The pulse energy also increases almost in the same pattern as the output power from 0.52 nJ to 0.91 nJ. Additionally, Fig. 6(b) shows the peak power in relation to the pump power, that also increases from 8.46 mW to a maximum of 14.79 mW.

Fig. 7 shows the TDFL mode-locked characteristics, analyzed at the maximum pump power of 967 mW. The TDFL mode-locked started to self-generate as the pump power increased from 821 mW to a maximum of 967 mW. Fig. 7(a) illustrates the pulses train of the TDFL mode-locked with a peak-to-peak separation of 128 ns, that corresponds to a repetition rate of 8.10 MHz. As seen, the pulses train is quite stable with a constant pulse width of 61.27 ns. By considering the time-bandwidth product (TBP) for a sech^2 shape as 0.315 as well as the obtained 3 dB spectral width (in frequency space) as 0.14 nm (11.63 GHz), the minimum possible pulse width is calculated as 27 ps. Fig. 7(b) shows the fundamental frequency of the TDFL mode-locked with a repetition rate of 8.10 MHz and the corresponding SNR of 23.76 dB. With a single repetition rate observed in the frequency domain, it can be concluded that the generated waveform is a cosine wave. This also suggests that the obtained mode-locked TDFL has a single longitudinal mode oscillating at 8.10 MHz which also corresponds to a single cavity round trip time. Due to this reason, the generated pulse duty cycle (PDC) seems to be quite large. Unlike the Q-switched fiber laser, where the pulse repetition rate is tunable within a certain pump power range, the mode-locked fiber laser possesses a constant repetition rate that is fixed by its cavity length.

The obtained pulsed fiber laser near the 2 μm region has good potentials in many scientific applications including remote sensing, spectroscopy and medicine. A few gas molecules such as carbon dioxide (CO_2) and hydrogen bromide (HBr) have absorption lines within this region, thus creating possibilities of designing cost-efficient gas tracing and sensing unit [30]. In addition to that, the presence of high-water absorption within this wavelength range also makes this kind of pulsed laser greatly desirable as a precise biological tissue ablation device [31].

5. Conclusion

We have successfully demonstrated both Q-switched and mode-locked fiber lasers with a ring TDFL cavity using NiO nanoparticles thin film SA. A stable Q-switched laser was established as the pump power increased to 528 mW and disappeared when the pump power raised beyond 711 mW. The Q-switched pulse had a maximum repetition rate and pulse energy of 19.58 kHz and 0.31 μJ, respectively. By adding a short length of Sc-DF to induce sufficient dispersion and nonlinearity in the cavity, self-starting mode-locked TDFL was observed at the threshold pump power of 821 mW. The mode-locked laser had a central wavelength of 1900.52 nm and a consistent repetition rate of 8.10 MHz. The pulse width was 51.27 ns, while the calculated maximum pulse energy was 0.91 nJ. These results show that the NiO can be an alternative SA material for generating a reliable and stable pulsed fiber laser, particularly in the 2.0 μm wavelength region.

References

[1] W. Gong, T.H. Chyba, D.A. Temple, Eye-safe compact scanning LIDAR technology, Opt. Lasers Eng. 45 (2007) 898–906.

[2] S. Ishii, K. Mizutani, H. Fukuoka, T. Ishikawa, B. Philippe, H. Iwai, T. Aoki, T. Itabe, A. Sato, K. Asai, Coherent 2 μm differential absorption and wind lidar with conductively cooled laser and two-axis scanning device, Appl. Opt. 49 (2010) 1809–1817.

[3] G.J. Koch, J.Y. Beyon, B.W. Barnes, M. Petros, J. Yu, F. Amzajerdian, M.J. Kavaya, U.N. Singh, High-energy 2 μm doppler lidar for wind measurements, Opt. Eng. 46 (2007) 116201.

[4] N.M. Fried, K.E. Murray, High-power thulium fiber laser ablation of urinary tissues at 1.94 μm, J. Endourology 19 (2005) 25–31.

[5] J. Geng, Q. Wang, Y. Lee, S. Jiang, Development of eye-safe fiber lasers near 2 μm, IEEE J. Sel. Top. Quantum Electron. 20 (2014) 150–160.

[6] Y. Meng, Y. Li, Y. Xu, F. Wang, CaRbon nanotube mode-locked thulium fiber laser with 200 nm tuning range, Sci. Rep. 7 (2017) 45109.

[7] D. Ma, Y. Cai, C. Zhou, W. Zong, L. Chen, Z. Zhang, 37.4 fs pulse generation in an Er: fiber laser at a 225 MHz repetition rate, Opt. Lett. 35 (2010) 2858–2860.

[8] M. Andrés, J. Cruz, A. Díez, P. Pérez-Millán, M. Delgado-Pinar, Actively q-switched all-fiber lasers, Laser Phys. Lett. 5 (2007) 93.

[9] H.Y. Ryu, H.S. Moon, H.S. Suh, Optical frequency comb generator based on actively mode-locked fiber ring laser using an acousto-optic modulator with injection-seeding, Opt. Express. 15 (2007) 11396–11401.

[10] M. Rahman, A. Latiff, U. Zaidi, M. Rusdi, A. Rosol, A. Bushroa, K. Dimyati, S. Harun, Q-switched and mode-locked thulium-doped fiber laser with pure antimony film saturable absorber, Opt. Commun. 421 (2018) 99–104.

[11] B. Posada-Ramirez, M. Durán-Sánchez, R. Alvarez-Tamayo, J. Alaniz-Baylón, B. Ibarra-Escamilla, R. Lopez-Estopier, E. Kuzin, All-fiber multi-wavelength passive Q-switched Er/Yb fiber laser based on a Tm-doped fiber saturable absorber, Laser Phys. 27 (2017) 035103.

[12] B. Ibarra-Escamilla, M. Durán-Sánchez, R.I. Álvarez Tamayo, B. Posada-Ramírez, P. Prieto-Cortés, J. Alaniz-Baylón, H. Santiago-Hernández, M. Bello-Jiménez, E.A. Kuzin, All-fiber laser with simultaneous Tm 3+ passive Q-switched and Ho 3+ gain-switched operation, Opt. Lett. 43 (2018) 3377–3380.

[13] B. Ibarra-Escamilla, M. Durán-Sánchez, B. Posada-Ramírez, R.I. Álvarez Tamayo, J. Alaniz-Baylón, M. Bello-Jiménez, P. Prieto-Cortés, E.A. Kuzin, Passively Q-Switched thulium-doped fiber laser using alcohol, IEEE Photonics Technol. Lett. 30 (2018) 1768–1771.

[14] X. Wang, P. Zhou, X. Wang, H. Xiao, Z. Liu, Pulse bundles and passive harmonic mode-locked pulses in tm-doped fiber laser based on nonlinear polarization rotation, Opt. Express 22 (2014) 6147–6153.

[15] M. Ismail, S. Tan, N. Shahabuddin, S.W. Harun, H. Arof, H. Ahmad, Performance comparison of mode-locked erbium-doped fiber laser with nonlinear polarization rotation and saturable absorber approaches, Chin. Phys. Lett. 29 (2012) 054216.

[16] U. Keller, K.J. Weingarten, F.X. Kartner, D. Kopf, B. Braun, I.D. Jung, R. Fluck, C. Honninger, N. Matuschek, J.A. Der Au, Semiconductor saturable absorber mirrors (sesam's) for femtosecond to nanosecond pulse generation in solid-state lasers, IEEE J. Sel. Top. Quantum Electron. 2 (1996) 435–453.

[17] M. Hisyam, M. Rusdi, A. Latiff, S. Harun, PMMA-Doped cdse quantum dots as saturable absorber in a q-switched all-fiber laser, Chin. Opt. Lett. 14 (2016) 081404.

[18] Z. Luo, D. Wu, B. Xu, H. Xu, Z. Cai, J. Peng, J. Weng, S. Xu, C. Zhu, F. Wang, Two-dimensional material-based saturable absorbers: towards compact visible-wavelength all-fiber pulsed lasers, Nanoscale 8 (2016) 1066–1072.

[19] Y. Chen, G. Jiang, S. Chen, Z. Guo, X. Yu, C. Zhao, H. Zhang, Q. Bao, S. Wen, D. Tang, Mechanically exfoliated black phosphorus as a new saturable absorber for both q-switching and mode-locking laser operation, Opt. Express. 23 (2015) 12823–12833.

[20] A.C. Ferrari, F. Bonaccorso, V. Fal'Ko, K.S. Novoselov, S. Roche, P. Bøggild, S. Borini, F.H. Koppens, V. Palermo, N. Pugno, Science and technology roadmap for graphene, related two-dimensional crystals, and hybrid systems, Nanoscale 7 (2015) 4598–4810.

[21] M.B. Hisyam, M.F.M. Rusdi, A.A. Latiff, S.W. Harun, Generation of mode-locked ytterbium doped fiber ring laser using few-layer black phosphorus as a saturable absorber, IEEE J. Sel. Top. Quantum Electron. 23 (2017) 39–43.

[22] M. Rusdi, A. Latiff, E. Hanafi, M. Mahyuddin, H. Shamsudin, K. Dimyati, S. Harun, Molybdenum disulphide tape saturable absorber for mode-locked double-clad ytterbium-doped all-fiber laser generation, Chin. Phys. Lett. 33 (2016) 114201.

[23] A. Latiff, M. Rusdi, M. Hisyam, H. Ahmad, S. Harun, A generation of 2 μm Q-switched thulium-doped fibre laser based on anatase titanium (IV) oxide film saturable absorber, J. Modern Opt. 64 (2017) 187–190.

[24] A. Nady, M.H.M. Ahmed, A.A. Latiff, A. Numan, C.R. Ooi, S.W. Harun, Nickel oxide nanoparticles as a saturable absorber for an all-fiber passively q-switched erbium-doped fiber laser, Laser Phys. 27 (2017) 065105.

[25] I.A.M. Alani, M.Q. Lokman, M.H.M. Ahmed, A.H.H. Al-Masoodi, A.A. Latiff, S.W. Harun, A few-picosecond and high-peak-power passively mode-locked erbium-doped fibre laser based on zinc oxide polyvinyl alcohol film saturable absorber, Laser Phys. 28 (2018).

[26] J. Wang, P. Yang, X. Wei, Z. Zhou, Preparation of nio two-dimensional grainy films and their high-performance gas sensors for ammonia detection, Nanoscale Res. Lett. 10 (2015) 119.

[27] Z. Tian, K. Wu, L. Kong, N. Yang, Y. Wang, R. Chen, W. Hu, J. Xu, Y. Tang, Mode-locked thulium fiber laser with MoS2, Laser Phys. Lett. 12 (2015) 065104.

[28] H. Liu, A.-P. Luo, F.-Z. Wang, R. Tang, M. Liu, Z.-C. Luo, W.-C. Xu, C.-J. Zhao, H. Zhang, Femtosecond pulse erbium-doped fiber laser by a few-layer MoS 2 saturable absorber, Opt. Lett. 39 (2014) 4591–4594.

[29] Z. Wang, H. Mu, J. Yuan, C. Zhao, Q. Bao, H. Zhang, Graphene-bi2te3 heterostructure as broadband saturable absorber for ultra-short pulse generation in er-doped and yb-doped fiber lasers, IEEE J. Sel. Top. Quantum Electron. 23 (2017) 195–199.

[30] W. Zeller, L. Naehle, P. Fuchs, F. Gerschuetz, L. Hildebrandt, J. Koeth, DFB Lasers between 760 nm and 16 μm for sensing applications, Sensors 10 (2010) 2492–2510.

[31] K. Scholle, S. Lamrini, P. Koopmann, P. Fuhrberg, 2 μm Laser sources and their possible applications, in: Frontiers in Guided Wave Optics and Optoelectronics, InTech, 2010.